



Title	Design of a high-temperature and high-pressure liquid flow cell for x-ray absorption fine structure measurements under catalytic reaction conditions
Author(s)	Kawai, Toshihide; Chun, Wang-Jae; Asakura, Kiyotaka; Koike, Yuichiro; Nomura, Masaharu; Bando, Kyoko K.; Oyama, S. Ted; Sumiya, Hitoshi
Citation	Review of Scientific Instruments, 79(1), 014101 https://doi.org/10.1063/1.2829156
Issue Date	2008-01-28
Doc URL	http://hdl.handle.net/2115/33047
Rights	Copyright 2008 American Institute of Physics. This article may be downloaded for personal use only. Any other use requires prior permission of the author and the American Institute of Physics.
Type	article
File Information	RevSciInstrum_79_014101.pdf



[Instructions for use](#)

Design of a high-temperature and high-pressure liquid flow cell for x-ray absorption fine structure measurements under catalytic reaction conditions

Toshihide Kawai, Wang-Jae Chun, and Kiyotaka Asakura^{a)}

Catalysis Research Center, Hokkaido University, Kita 21-10, Kita-ku, Sapporo 001-0021, Japan

Yuichiro Koike and Masaharu Nomura

Photon Factory, Institute of Structure Material Science, High Energy Accelerator Research Organization (KEK-PF), Oho 1-1, Tsukuba 305-0811, Japan

Kyoko K. Bando

National Institute of Advanced Industrial Science and Technology, 16-1, Onogawa, Tsukuba 305-8562, Japan

S. Ted Oyama

Environmental Catalysis and Materials Laboratory, Departments of Chemical Engineering and Chemistry, Virginia Polytechnic Institute and State University, Blacksburg, Virginia 24061-0211, USA

Hitoshi Sumiya

Electronics & Materials R&D Laboratories, Sumitomo Electric Industry, Konyo Kita 1-1-1, Itami 664-0016, Japan

(Received 19 June 2007; accepted 5 December 2007; published online 28 January 2008)

The design and performance of a new high-pressure and high-temperature cell for measurement of x-ray absorption fine structure (XAFS) spectra of solid catalysts working in a flowing liquid are presented. The cell has flat, high-purity sintered cubic boron nitride (*c*-BN) windows which can tolerate high temperature (900 K) and high pressure (10 MPa). The *c*-BN is a new material which has the highest tensile strength, second only to diamond, and is also chemically and thermally stable. The use of the cell is demonstrated for measurements of PtPd/Al₂O₃ and Ni₂P/SiO₂ hydrodesulfurization catalysts at reaction conditions. A technique called $\Delta\chi$ ($\Delta\chi$), involving determining the difference between XAFS spectra of the sample at reaction conditions and the bare sample, is introduced. © 2008 American Institute of Physics.

[DOI: 10.1063/1.2829156]

INTRODUCTION

Since the structure of catalysts can change during reaction, it is important to characterize them under real working conditions to shed light on reaction mechanisms and activation and deactivation processes.¹ X-ray absorption fine structure (XAFS) measurements in the form of extended (EXAFS) and near-edge (XANES) spectroscopies applied at *in situ* conditions are powerful tools to obtain local geometric and electronic information about x-ray absorbing atoms at reaction conditions. Since x-rays are deeply penetrating, they can be used to measure XAFS spectra even in the presence of gaseous reactants and products. There have been many XAFS studies performed at *in situ* reaction conditions reported since the 1970s. For example, Lytle *et al.* first applied *in situ* XAFS techniques to study the preparation process of Ru clusters on a SiO₂ support and their structural conversion by treatment with O₂.² Koningsberger found dynamic changes in the structure of Rh clusters after adsorption of CO.³ Iwasawa *et al.* proposed a new reaction mechanism, denoted as metal-promoted CO insertion, by *in situ* XAFS observations of Rh dimer catalysts interacting with CO.⁴ In addition, time-resolved *in situ* XAFS gives fruitful informa-

tion about reaction intermediates.⁵ Many catalytic reactions are carried out in the gas phase at high pressure, and *in situ* XAFS has been developed for these conditions. The structural changes of Co in the presence of high-pressure oxygen was studied by XAFS and it was demonstrated that Co–O–Co species were quite active for the room temperature oxidation reaction.⁶ For *in situ* XAFS studies of gas-phase reactions, the x-ray windows can be placed a distance away from the hot sample zone and can be cooled by water since x-rays are not attenuated much by gases, which have low densities and do not absorb x-ray strongly. Hence, in gas-phase applications, windows need to only tolerate high pressure. Bando *et al.* successfully measured XAFS spectra of Rh/NaY catalysts under high pressures of CO₂ and H₂ using plastic windows which could be used at temperatures lower than 400 K.⁷

Hydrodesulfurization (HDS) is an important catalytic reaction used to reduce the sulfur content in fossil fuels.⁸ Recently enacted severe environmental regulations require the development of high performance HDS catalysts.⁹ NiMoS and CoMoS are typical commercial catalysts used in HDS and *in situ* XAFS techniques have been applied to study their preparation process and performance in gas-phase model reactions.^{10–12} However, industrial hydrodesulfurization reactions are carried out at high pressure in the presence of liquid

^{a)} Author to whom correspondence should be addressed. Electronic mail: askr@cat.hokudai.ac.jp.

TABLE I. The *in situ* XAFS cells applicable to high-pressure and high-temperature liquid-phase catalytic reactions.

Authors	Cell type	Window	Target	Performance	Reference
B.S. Clausen	Capillary type	0.4 mm OD quartz	Cu catalyst for methanol synthesis	Gas phase	13
D.A. DallaBetta	Cell, liquid film		MoS ₂	14 MPa, 700 K	36
S. L. Wallen <i>et al.</i>	Capillary type	0.36 mm OD silica	SCF ^a solution	311.5 K, 1.6 MPa, hair pin type	37
D.G. Barton	Capillary type	1.0 mm OD quartz	Catalyst	Gas phase	38
F.S. Modica	Capillary type	5 mm OD Be tube	Catalyst	600 °C, 6.89 MPa gas phase	18 and 19
K. Nishikawa <i>et al.</i>	Cell type	Φ4 mm, 0.4 mm' diamond	SAXS ^b of CF ₃ HSCF	333 K, 15 MPa	39 and 40
J.L. Fulton	Cell type	0.5 mm' diamond	XAFS, Cu <i>K</i> edge	598 K batch	41
A. M. J. van der Eerden	Cell type	0.007 mm' Be	Low energy XAFS, gas phase	0.1 MPa, 80–750 K	42
M. M. Hoffman	Cell type	Φ3 mm, 1 mm' diamond	WO ₄ ²⁻ solution	873 K, 150 MPa	43
J.L. Fulton	Cell type	Φ0.3 mm, 0.75 mm' diamond	Ca and Cl <i>K</i> edge, XAFS	773 K, 100 MPa	44
J. Grunwaldt	Cell type	5 × 1 mm ² , 0.5 mm' Be	Zn base	500 K, 25 MPa	20
J. Grundwald	Review paper				45
C. Roth	Cell type	Graphite	Pt <i>L</i> edge XAFS, Fuel cell	373 K, 0.1 MPa	46
W.A. Basset	Diamond anvil cell	Diamond		933 K, 800 MPa	47
J. Grundwald	Cell type	1 mm' Be	Pd <i>K</i> edge	473 K, 20 MPa	48

^aSCF=supercritical fluid.

^bSAXS=small angle x-ray scattering.

oil at about 3 MPa and 600 K. *In situ* XAFS work under these real HDS conditions is quite difficult because liquid oil has 1000 times higher density than typical gases and absorbs x-rays strongly. For example, a 1 cm thick layer of liquid-phase hydrocarbon such as *n*-octane has an absorbance of $\mu\tau \approx 4$ in the 8 keV region which is comparable to that of a typical solid to be examined. Because of the need to minimize the optical path length, windows are required to be placed very close to the sample, but this creates formidable problems for their cooling. This leads to the conclusion that windows must *simultaneously* withstand *high-pressure and high-temperature* conditions. In addition, the windows must be chemically stable under these severe conditions. Several windows and cells have been proposed for *in situ* XAFS measurements in the presence of liquids but have problems that will be addressed later. In this paper we present a new type of window material—a high-purity binderless polycrystalline *c*-BN, which can withstand harsh environments. Successful measurement of XAFS spectra of Ni₂P/SiO₂ for HDS under liquid-phase flow conditions is presented.

STRATEGY FOR THE DESIGN OF AN *IN SITU* XAFS CELL

Table I summarizes the characteristics of *in situ* cells that have been used for liquid-phase studies. The cells are classified into two types. The first type of cell is of a tubular design in which measurements are made through the tube wall. The second type of cell is a chamber-type device in which measurements are made through a flat window placed in the neighborhood of the sample.

The first type of cell often utilizes quartz tubing, as employed in high-pressure liquid chromatography (HPLC) capillary columns. The cylindrical geometry is advantageous because it can reduce stresses on the wall.^{13–16} The tubular-type

cell, however, has optical deficiencies. The curved windows give rise to inhomogeneous thickness effects because x-rays experience greater attenuation passing through the center than through the edges, and this deteriorates the accuracy of the XAFS amplitude information.¹⁷ A cell consisting of a thick Be tube has been recently described,^{18,19} but Be poses grave safety concerns. At high temperature, Be forms an oxide which can flake off and pose danger to the user because of the extreme toxicity of Be.

The second type of cell has flat windows attached to an enclosure that holds the sample. Window materials that have been used are Be and diamond. Grunwaldt *et al.* recently reported a high-pressure XAFS cell with Be/PEEK [poly(etherether ketone)] windows that could withstand 25 MPa and 500 K.²⁰ However, as mentioned above, Be is a poor window material because of its toxicity and tendency to form an oxide. Diamond as a window material is thermally and physically stable but prohibitively expensive. For these reasons, a new window material is desirable. The window material for liquid-phase XAFS measurements should have the following properties: (1) it should be chemically and thermally stable; (2) It should withstand high pressure (10 MPa); (3) it should transmit x-rays with small absorption, $\mu\tau < 3$; and (4) it should be amenable to fabrication in sizes larger than 3 mm in diameter.

This paper reports the construction of a new type of *in situ* cell which uses binderless polycrystalline *c*-BN for its windows.^{21,22} The binderless *c*-BN is a new material for x-ray windows which possesses desirable properties such as chemical and thermal stability. Moreover, *c*-BN is the second hardest materials next to diamond. The tensile strength of *c*-BN is 1080 MPa while those of diamond and Be are 2000 MPa and 200 MPa, respectively. Conventional *c*-BN compacts are sintered from *c*-BN powder under

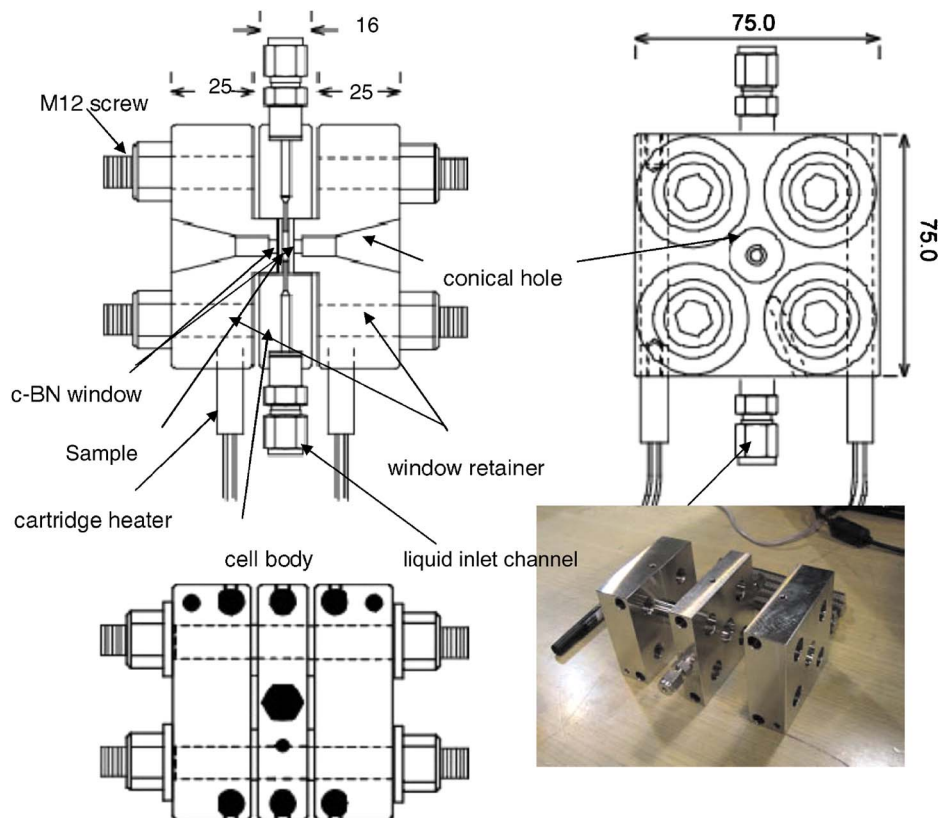


FIG. 1. (Color online) Schematic diagram of the *in situ* cell.

4.5–5.5 GPa and 1473–1673 K in the presence of 10–50 vol % metal or ceramic binders which affect its hardness and x-ray transmission properties. The binderless *c*-BN is directly transformed from a high-purity hexagonal BN (whose main impurity is B_2O_3 and is present at less than 0.02 wt %) at high temperature (2400 K) and pressure (7.7 GPa). The binderless polycrystalline *c*-BN has a hardness of about 50 GPa and a transverse rupture strength of 1–1.5 GPa.²³ The high purity of the material is an important feature because impurities, particularly if they happen to have an atomic number just above the element being observed, will interfere with the EXAFS oscillations of the element.

The thickness necessary to tolerate a hydrostatic pressure P is given by the Roark formula,²⁴

$$\sigma_{\max} = \frac{3}{8}P(3 + \nu)\left(\frac{r}{d}\right)^2, \quad (1)$$

where σ_{\max} , ν , d , and r are the maximum tensile strength, Poisson ratio, thickness, and radius, respectively. The required thicknesses to withstand 3 MPa for a 3 mm radius window fall in the order: diamond < *c*-BN < Be < Al_2O_3 < SiO_2 with respective thicknesses 0.21 < 0.43 < 0.54 < 0.55 < 0.96 mm. A safety factor of 6 was used for diamond, *c*-BN, Al_2O_3 , and SiO_2 and of 4 for Be.

The cell constructed in this study used 800 μ m thick *c*-BN windows, which can tolerate a pressure of 10 MPa and can give sufficient transmittance for x-rays at around 8 keV (Ni *K*-edge region).

Other positive features of *c*-BN are the following: (1) *c*-BN is thermally (1625 K) and chemically more stable than diamond; (2) *c*-BN has a large thermal conductivity

(400 $W m^{-1} K^{-1}$); (3) *c*-BN is nontoxic and economical; and (4) *c*-BN has negligible gas permeability. No passage of H_2 or He could be detected even at 5 MPa. In conclusion, *c*-BN is a highly suitable material for the construction of XAFS windows for high-temperature and high-pressure applications.

Other windows

If temperatures are less than 600 K for pretreatments and reactions, windows made of engineering plastics may be used. Tests of two engineering polymers were carried out to determine their performance and feasibility for use as window materials. Polybenzimidazole is one candidate, with a tensile strength of 160 MPa and flammability tolerance. Its glass transition temperature is 708 K. Polyimide is another candidate which can be used at temperatures lower than 573 K. The thicknesses required to tolerate 10 MPa pressure are 0.85 and 1.2 mm for polybenzimidazole and polyimide, respectively. The attenuation lengths in the 8 keV region are approximately 1 mm. Consequently, both materials have enough strength and x-ray transmittance. The use of polybenzimidazole windows for *in situ* XAFS measurement of a PtPd/USY (ultra stable zeolite) catalyst is given as an example later.

Construction of the *in situ* cell

Figure 1 shows a diagram of the *in situ* cell. The cell body is made of stainless steel SS316 which is more sulfur tolerant than SS304. The body is composed of three parts. The lateral parts are window retainers which push the windows strongly against the central body using four M12

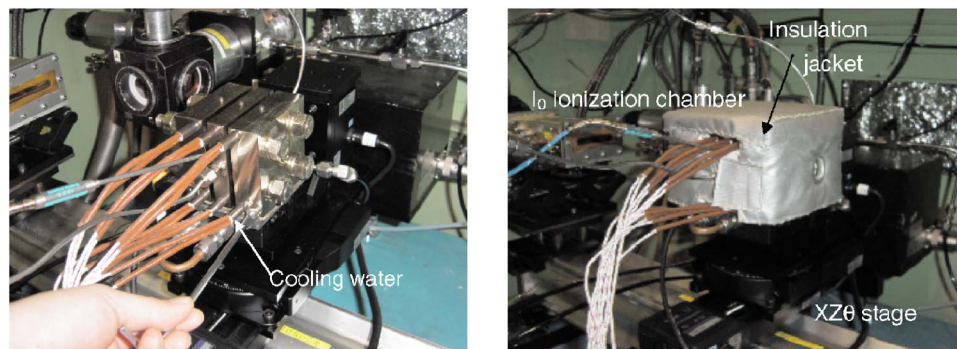


FIG. 2. (Color online) XAFS cell in the synchrotron hut.

screws. Conical holes at the center of the window retainers allow the passage of the x-rays. The holes are 3 mm wide at the window side and 10 mm wide at the air end. The central body of the cell has a 2 mm thick bore of 9 mm diameter which contains the sample. The bore has two small channels of 1 mm diameter at either side which are connected to the liquid/gas inlet and outlet ports, respectively. The cell is heated homogeneously using six cartridge heaters (200 V, 200 W each), and the whole cell is covered with a thermal insulation jacket, as shown in Fig. 2. The temperatures of both the window retainers and central body are monitored by thermocouples.

The cell is mounted on a four-axis stage with rotation, tilt, and yz motion, as shown in Fig. 2. This allows easy positioning of the sample in the optical path. To prevent fracturing the *c*-BN by uneven loading, it is welded by silver brazing onto a SS316 flange which is sandwiched by 0.3 mm thick Cu gaskets on both sides. The coefficients of thermal expansion of *c*-BN and SS316 are different (4.3×10^{-6} and $14.7 \times 10^{-6} \text{ K}^{-1}$) so that the temperature is increased and decreased slowly (1.5 K/min).

GAS AND LIQUID FEED SYSTEM

Figure 3 shows the high-pressure oil feeding system. High pressure is loaded by the gas pressure of H_2 and is adjusted by a back pressure control regulator (N15T-3A-G1, Tama Seiki Co.). H_2 flow rate is controlled by digital mass

flow controllers (5850E, Honma Riken). The liquid oil is pumped into the H_2 flow using a double-plunger-type high-pressure pump (LP6300 S324, LaboCotek). The exhausted oil is gathered in the oil trap. H_2S is trapped with NaOH solution and ZnO. The pressure stability is about 1%. Because the absorbance of gas phase and the compressibility of the oil are small enough, the 1% pressure precision little affects our data. Thus, we can measure the EXAFS when H_2 flow rate is high enough (more than about 10 ml/min with 2 g/h oil supply) and oil and H_2 are well mixed. However, when the H_2 flow becomes slower, oil and H_2 are ill mixed and periodic glitches appear in the XAFS spectra owing to the pulsating oil flow. In this case, we have to change the accumulation time to avoid the glitches in the EXAFS region or stop the feed.

XAFS MEASUREMENTS

XAFS measurements were carried out at BL-7C of the Photon Factory, Institute of Material Structure Science (KEK-IMSS-PF). The energy and the current of the storage ring were 2.5 GeV and 400 mA, respectively. The beam was monochromatized with a Si(111) double crystal monochromator and was focused on the sample by sagittal focusing of the second Si(111) crystal. The incident and transmitted intensities were monitored by ion chambers filled with N_2 and N_2/Ar (75/25), respectively. Higher harmonics were removed by 70% detuning of the parallelism of the two Si(111) crystals.

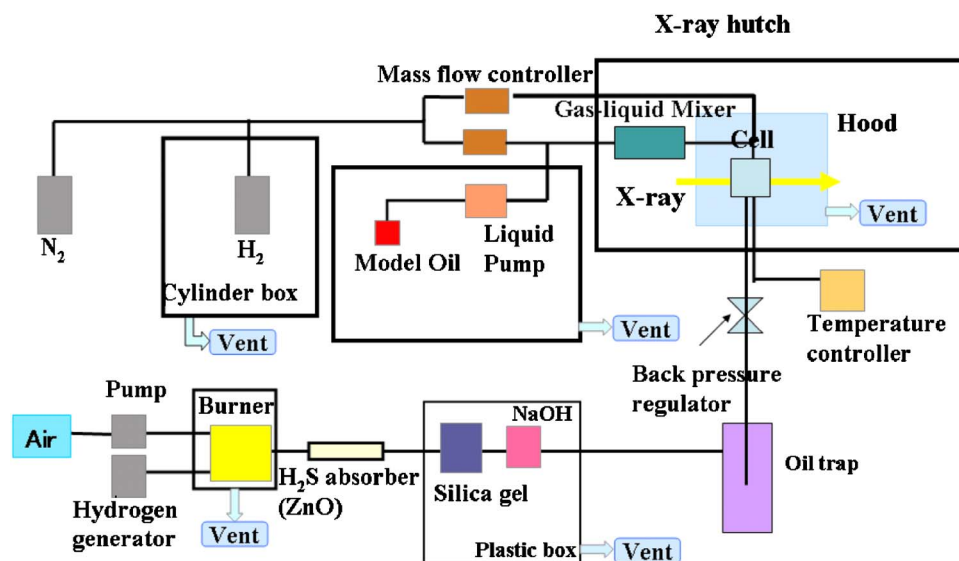


FIG. 3. (Color online) A high-pressure oil feeding system.

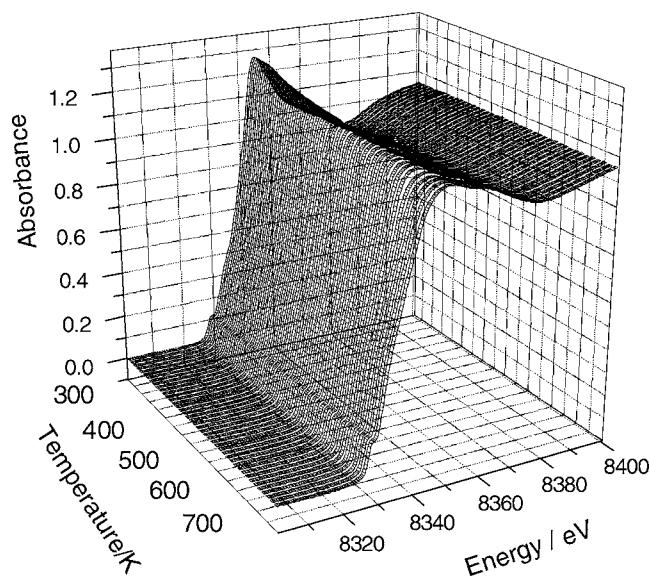


FIG. 4. Changes in XANES spectra during the reduction process up to 723 K.

RESULTS AND DISCUSSION

In situ XAFS of Ni₂P on SiO₂ using *c*-BN windows

Ni₂P/SiO₂ is a highly active hydrotreating catalyst employed in hydrodesulfurization (HDS) and hydrodenitrogenation (HDN) of fossil fuels.^{25–29} Ni₂P is first activated by reduction in H₂ at 723 K. The HDS reaction is usually carried out at 613 K and 3 MPa in the presence of liquid oil. These conditions make necessary the use of *c*-BN windows. Ni₂P supported on SiO₂ was prepared as described before.³⁰ For the measurement, a quantity of 16 mg Ni₂P/SiO₂ was loaded in the cell and heated at 1.5 K/min to 723 K under 50 ml/min of H₂ flow. Figure 4 shows the (XANES) spectra during the reduction process. The reduction process roughly occurred in two steps. In the first step at less than 500 K, the first edge peak was reduced gradually suggesting the removal of OH or H₂O ligands. In the second step at around 700 K, the formation of the Ni₂P structure occurred as indicated by the appearance of a peak at 8360 eV. After the reduction was completed, the sample was cooled to room temperature to measure room temperature XAFS spectra and was heated again to the reaction temperature of 613 K in a H₂ flow. In these heating and cooling processes, we could not find any leakage of hydrogen due to the expansion and contraction of the cell. The H₂ pressure was raised to 3 MPa and the flow rate was 40 ml/min. The model oil [20 wt % tetralin and 77 wt % tetradecane with 3 wt % dibenzothiophene (DBT) corresponding to a sulfur level of 5900 ppm] was added to the flow. The oil feed rate was 2 g/h. Figure 5 shows the oscillation $\chi(k)$ in the EXAFS region of Ni₂P/SiO₂ before and 10 h after oil introduction. The spectra were recorded at 3 MPa and 613 K. Although the total absorbance was changed, the spectrum after background removal and normalization for the edge height showed similar oscillations to that before the reaction, as shown in Figs. 5(a) and 5(b). Background distortion of the spectra owing to the strong absorption by the oil was not observed. These observations indicated that the spectra before and during the reac-

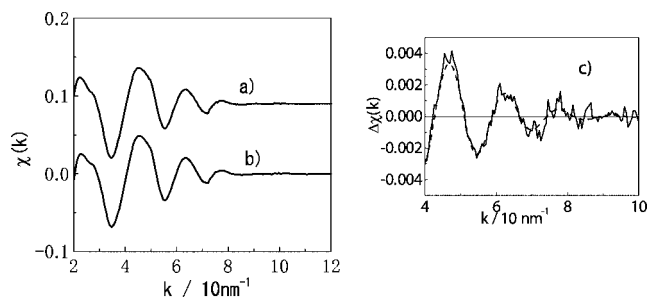


FIG. 5. Illustration of the $\Delta\chi$ technique. $\chi(k)$ oscillations of the Ni *K*-edge EXAFS for Ni₂P/SiO₂ before (a) and 10 h after the HDS reaction (b) and their difference spectrum $\Delta\chi$ (c). Broken line is best fit curve assuming a Ni–S bond of 0.228 nm.

tion could be subtracted to elucidate the small changes in the catalyst as it carried out the hydrodesulfurization of DBT. This method is denoted as $\Delta\chi$ in reference to an analogous techniques called as different file³¹ and $\Delta\mu$.^{32–34} Using the $\Delta\chi$ technique a distinctive oscillation was observed in the difference spectrum under the reaction conditions as shown in Fig. 5(c). Curve fitting analysis of this oscillation gives a bond distance corresponding to Ni–S bonds (0.228 nm). This indicates that the active phase of the catalyst is a phosphosulfide during the HDS reaction.²⁸ In summary the *c*-BN window allows *in situ* XAFS measurements under difficult HDS working conditions. The $\Delta\chi$ technique works well because the signal from the underlying bulk bonds in the Ni₂P nanoparticles cancel, leaving behind the information from the new surface bonds.

In situ XAFS of PtPd in USY zeolite

PtPd cluster in USY zeolite³⁵ is another type of HDS active catalyst. PtPd clusters were reduced at 573 K for 1 h under a flow of H₂ with a flow rate 50 cm³/min. Then the cell was pressurized to 4 MPa and a model oil, composed of dibenzothiophene (sulfur=500 ppm), tetralin (20 wt %) and hexadecane (as a solvent), was introduced at the rate of 4 g/h with H₂ (whose flow rate was set at 40 ml/min). Measurements of the sample were carried out with plastic polybenzimidazole windows, 3 mm thick. Figure 6 shows the XAFS oscillations and their Fourier transforms for the PtPd clusters in USY. The reaction was continued for 24 h. Before the reaction Pt and Pd were both in a reduced metallic state. Soon after the reaction started, the Pt and Pd both were sulfided and after the 24 h Pt–S and Pd–S bonds were clearly visible. These measurements demonstrate that XAFS measurements can be carried out using plastic windows under high-pressure liquid reaction condition as long as the process does not require temperatures higher than 553 K.

CONCLUSIONS

Measurement of XAFS spectra during difficult HDS reaction conditions (3 MPa, 613 K) were made using a new type of x-ray transparent flat window material, cubic boron nitride (*c*-BN) which is nontoxic, inexpensive, and stable. The cell may be utilized for a wide variety of catalytic reactions performed under high pressure and high temperature in

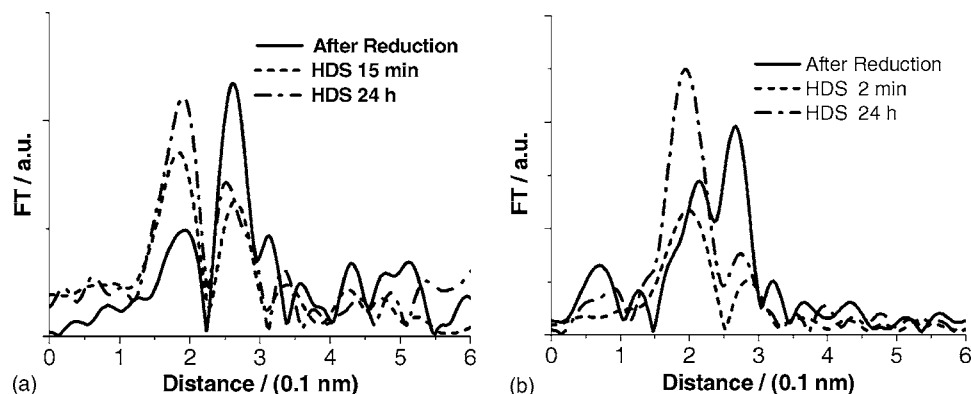


FIG. 6. Fourier transform of Pd K -edge (a) and Pt L_{3} -edge (b) EXAFS oscillations [$k^3\chi(k)$] under the HDS conditions.

the presence of a liquid phase. A technique called $\Delta\chi$ was introduced which allows identification of new chemical bonds formed in a working catalyst.

ACKNOWLEDGMENTS

We appreciate Dr. K. Takahashi (Kanazawa University) for his advice about the design of the high-temperature and high-pressure cell. The XAFS measurement was carried out under the approval of PF-PAC (2001G297, 2003G247, and 2006G109). This work is financially supported by Grant-in-Aid for Scientific Research category S (No. 16106010), and the U.S. Department of Energy.

¹J. F. Haw, *In situ Spectroscopy in Heterogeneous Catalysis* (Wiley-VCH, Weinheim, 2002).
²F. W. Lytle, G. H. Via, and J. H. Sinfelt, *J. Chem. Phys.* **67**, 3831 (1977).
³H. F. J. Van't Blik and R. Prins, *J. Catal.* **97**, 188 (1986).
⁴K. Asakura, K. K. Bando, K. Isobe, H. Arakawa, and Y. Iwasawa, *J. Am. Chem. Soc.* **112**, 3242 (1990); K. Asakura, K. K. Bando, Y. Iwasawa, H. Arakawa, and K. Isobe, *ibid.* **112**, 9096 (1990).
⁵B. S. Clausen, J. Schiotz, L. Graback, C. V. Ovesen, K. W. Jacobsen, J. K. Norskov, and H. Topsoe, *Top. Catal.* **1**, 367 (1994); P. Kappen, J. D. Grunwaldt, B. S. Hammershoi, L. Troger, and S. Clausen, *J. Catal.* **198**, 56 (2001); G. Sankar, J. M. Thomas, D. Waller, J. W. Couves, C. R. A. Catlow, and G. N. Greaves, *J. Phys. Chem.* **96**, 7485 (1992); A. Yamaguchi, T. Shido, Y. Inada, T. Kogure, K. Asakura, M. Nomura, and Y. Iwasawa, *Bull. Chem. Soc. Jpn.* **74**, 801 (2001); A. Yamaguchi, A. Suzuki, T. Shido, Y. Inada, K. Asakura, M. Nomura, and Y. Iwasawa, *Catal. Lett.* **71**, 203 (2001); A. Suzuki, Y. Inada, A. Yamaguchi, T. Chirara, M. Yuasa, M. Nomura, and Y. Iwasawa, *Angew. Chem., Int. Ed.* **42**, 4795 (2003).
⁶K. Asakura and Y. Iwasawa, *J. Phys. Chem.* **93**, 4213 (1989).
⁷K. K. Bando, T. Saito, K. Kato, T. Tanaka, F. Dumeignil, M. Imamura, N. Matsubayashi, and H. Shimada, *J. Synchrotron Radiat.* **8**, 581 (2001).
⁸G. Ertl and H. Knozinger, *Handbook of Heterogeneous Catalysis* (VCH, Weinheim, 1997).
⁹R. Shafi and G. J. Hutchings, *Catal. Today* **59**, 423 (2000).
¹⁰T. Shido and R. Prins, *Curr. Opin. Solid State Mater. Sci.* **3**, 330 (1998); R. Cattaneo, T. Shido, and R. Prins, *J. Synchrotron Radiat.* **8**, 158 (2001).
¹¹H. Topsoe, *J. Catal.* **216**, 155 (2003).
¹²M. Shirai, N. Iwasa, K. K. Bando, and T. Kubota, *Catal. Today* **87**, 117 (2003).
¹³B. S. Clausen and H. Topsoe, *Catal. Today* **9**, 189 (1991).
¹⁴B. S. Clausen, L. Grabak, G. Steffensen, P. L. Hansen, and H. Topsoe, *Catal. Lett.* **20**, 23 (1993).
¹⁵G. Sankar, J. M. Thomas, D. Waller, J. W. Couves, C. R. A. Catlow, and G. N. Greaves, *J. Phys. Chem.* **96**, 7485 (1992).
¹⁶S. R. Bare, G. E. Mickelson, F. S. Modica, A. Z. Ringwelski, and N. Yang, *Rev. Sci. Instrum.* **77** (2006).
¹⁷E. A. Stern and K. Kim, *Phys. Rev. B* **23**, 3781 (1981).
¹⁸F. S. Modica, S. R. Bare, and G. E. Mickelson, in *Proceedings of the 18th NACS Meeting, Cancun, Mexico, 2003* (unpublished), p 210.
¹⁹S. R. Bare, N. Yang, S. D. Kelly, G. E. Mickelson, and F. S. Modica,

Proceedings of XAFS 13, USA, edited by B. Hedman and P. Pianetta, 2007 (unpublished), p. 622.
²⁰J. D. Grunwaldt, M. Ramin, M. Rohr, A. Michailovski, G. R. Patzke, and A. Baiker, *Rev. Sci. Instrum.* **76**, 054104 (2005).
²¹M. Akaishi, T. Satoh, M. Ishii, T. Taniguchi, and S. Yamaoka, *J. Mater. Sci. Lett.* **12**, 1883 (1993).
²²H. Sumiya, S. Uesaka, and S. Sato, *J. Mater. Sci.* **35**, 1181 (2000).
²³H. Sumiya, S. Uesaka, and S. Sato, *Proceedings of the 6th NIRIM International Symposium on Advanced Materials (ISAM'99)*, 1999 (unpublished), p. 13.
²⁴W. Beitz, *Handbook of Mechanical Engineering* (Springer, London, 1994).
²⁵S. T. Oyama, *J. Catal.* **216**, 343 (2003).
²⁶S. T. Oyama and Y. K. Lee, *J. Phys. Chem.* **109**, 2109 (2005).
²⁷S. T. Oyama, X. Wang, Y.-K. Lee, and W.-J. Chun, *J. Catal.* **221**, 263 (2004).
²⁸T. Kawai, K. K. Bando, Y. K. Lee, S. T. Oyama, W. J. Chun, and K. Asakura, *J. Catal.* **241**, 20 (2006).
²⁹T. Kawai, K. K. Bando, Y.-K. Lee, S. T. Oyama, W.-J. Chun, and K. Asakura, *AIP Conf. Proc.* **882**, 616 (2007).
³⁰S. T. Oyama, X. Wang, Y. K. Lee, K. Bando, and F. G. Requejo, *J. Catal.* **210**, 207 (2002).
³¹D. C. Koningsberger, J. B. A. D. van Zon, H. F. J. van't Blik, G. J. Visser, R. Prins, A. M. Mansour, D. E. Sayers, D. R. Short, and J. R. Katzer, *J. Phys. Chem.* **89**, 4075 (1985).
³²T. Kubota, K. Asakura, N. Ichikuni, and Y. Iwasawa, *Chem. Phys. Lett.* **256**, 445 (1996).
³³D. E. Ramaker, M. Teliska, Y. Zhang, A. Yu, and D. C. Koningsberger, *Phys. Chem. Chem. Phys.* **5**, 4492 (2003).
³⁴M. Teliska, V. S. Murthi, S. Mukerjee, and D. E. Ramaker, *J. Electrochem. Soc.* **152**, 1259 (2005).
³⁵K. K. Bando, T. Kawai, K. Asakura, T. Matusi, L. Le Bihan, H. Yasuda, Y. Yoshimura, and S. T. Oyama, *Catal. Today* **111**, 199 (2006).
³⁶R. A. Dalla Betta, M. Boudart, K. Fogar, D. Loffler, and J. Sanchezarrieta, *Rev. Sci. Instrum.* **55**, 1910 (1984).
³⁷S. L. Wallen, D. M. Pfund, J. L. Fulton, C. R. Yonker, M. Newville, and Y. Ma, *Rev. Sci. Instrum.* **67**, 2845 (1996).
³⁸D. G. Barton, S. L. Soled, G. D. Meitzner, G. A. Fuentes, and E. Iglesia, *J. Catal.* **181**, 57 (1999).
³⁹K. Nishikawa and M. Takematsu, *Jpn. J. Appl. Phys., Part 1* **32**, 5155 (1993).
⁴⁰K. Nishikawa and T. Morita, *J. Phys. Chem. B* **101**, 1413 (1997).
⁴¹J. L. Fulton, J. G. Darab, and M. M. Hoffmann, *Rev. Sci. Instrum.* **72**, 2117 (2001).
⁴²A. M. van der Eerden, J. A. van Bokhoven, A. D. Smith, and D. C. Koningsberger, *Rev. Sci. Instrum.* **71**, 3260 (2000).
⁴³M. M. Hoffmann, J. G. Darab, S. M. Heald, C. R. Yonker, and J. L. Fulton, *Chem. Geol.* **167**, 89 (2000).
⁴⁴J. L. Fulton, Y. Chen, S. M. Heald, and M. Balasubramanian, *Rev. Sci. Instrum.* **75**, 5228 (2004).
⁴⁵J. D. Grunwaldt and A. Baiker, *Phys. Chem. Chem. Phys.* **7**, 3526 (2005).
⁴⁶C. Roth, N. Martz, T. Buhrmester, J. Scherer, and H. Fuess, *Phys. Chem. Chem. Phys.* **4**, 3555 (2002).
⁴⁷W. A. Bassett, A. J. Anderson, R. A. Mayanovic, and I.-M. Chou, *Z. Kristallogr.* **215**, 711 (2000).
⁴⁸J.-D. Grunwaldt, M. Caravati, and A. Baiker, *J. Phys. Chem. B* **110**, 9916 (2006).